

Multi-dimensional numerical simulations of type Ia supernova explosions

F. K. Röpké

Max-Planck-Institut für Astrophysik
Karl-Schwarzschild-Str. 1, 85741 Garching, Germany

fritz@mpa-garching.mpg.de
www.mpa-garching.mpg.de/~fritz

Abstract

The major role type Ia supernovae play in many fields of astrophysics and in particular in cosmological distance determinations calls for self-consistent models of these events. Since their mechanism is believed to crucially depend on phenomena that are inherently three-dimensional, self-consistent numerical models of type Ia supernovae must be multi-dimensional. This field has recently seen a rapid development, which is reviewed in this article. The different modeling approaches are discussed and as an illustration a particular explosion model – the deflagration model – in a specific numerical implementation is presented in greater detail. On this exemplary case, the procedure of validating the model on the basis of comparison with observations is discussed as well as its application to study questions arising from type Ia supernova cosmology.

1 Introduction

The fact that many astrophysical processes are inherently three-dimensional makes realistic numerical simulations challenging. Although computational resources increase steadily, complex phenomena cannot be directly resolved in such simulations in the foreseeable future. Even exploiting the available computational power and memory, as most multi-dimensional astrophysical simulations do, considerable effort is required in modeling the processes in a way that despite the shortcomings in resolution the results provide credible physical approximations to the problems. Moreover, the implementation of efficient numerical techniques is one of the cornerstones of successful multi-dimensional modeling of astrophysical phenomena.

Type Ia supernovae (SNe Ia henceforth) are an excellent example for this class of astrophysical objects. Numerical simulations of these events in three dimensions easily reach the limits of today's computational resources. But as the underlying physical mechanism is believed to crucially depend on three-dimensional phenomena, such as turbulence, this is the only conceivable way towards self-consistent models of type Ia supernova explosions. Since Hillebrandt & Niemeyer (2000) reviewed type Ia supernova explosion models, the field has witnessed a brisk development. Progress in numerical methods and computational capabilities facilitated pioneering three-dimensional (3D) simulations, which will be reviewed in the following.

Self-consistent SN Ia models are called for in order to achieve a sound understanding of the mechanism of these astrophysical events. This is motivated by their significant impact on many aspects of astrophysics and cosmology. Being one of the main sources of iron group elements, SNe Ia contribute to the chemical evolution of galaxies (e.g. François et al., 2004). They affect star formation and drive shock waves in the interstellar and intergalactic media.

Most remarkable, however, was the application of SNe Ia in observational cosmology, where these objects were employed as distance indicators (as put forward by Branch & Tammann, 1992). Evidently, SNe Ia are a valuable tool to extend the Hubble diagram to large redshifts and to determine the Hubble constant (Hamuy et al., 1996; Branch, 1998). At redshifts above 0.5, a significant deviation from the linear Hubble law was noticed (Riess et al., 1998; Perlmutter et al., 1999). Here, SNe Ia appear dimmer than expected in a matter-dominated flat or open Friedmann-Robertson-Walker Universe. This led to the spectacular interpretation that the expansion of Universe is currently undergoing an acceleration. The determination of the driving force of this acceleration is one of the greatest challenges in contemporary physics. Meanwhile it is parametrized as “dark energy” (see e.g. Leibundgut, 2001). Determinations of cosmological parameters based on anisotropies in the cosmic microwave background radiation (Spergel et al., 2003) and on large-scale galaxy surveys provided independent confirmation of the SN Ia measurements.

Yet the question of the applicability of SNe Ia as distance indicators is still not satisfactorily answered. SNe Ia are remarkably uniform events by astrophysical standards, but evidently no standard candles. Only a calibration of the distance measurements according to empirical correlations between observables provides the necessary accuracy for the determination of cosmological parameters. A firm theoretical reasoning of such correlations is, however, still lacking.

The simplest form of dark energy is a cosmological constant, but more complicated contributions to the energy-momentum tensor in the Einstein equations are also conceivable. How can one determine the nature of the dark energy? A first step would be to constrain its equation of state. SNe Ia seem to be a suitable tool for this task and currently two major campaigns (Astier et al., 2005; Sollerman et al., 2005) apply them in distance determinations of hundreds of supernovae out to redshifts of $z \sim 1$ and systematic satellite-borne SN Ia observations are planned. The large number of observations is necessary to reduce the statistical errors because putting tight constraints on dark energy equation of state (see Astier et al., 2005, for recent results) requires a high accuracy of the distance determinations. But still, potential systematic errors arising from calibration of the distance measurements may obscure the results. Getting a handle on these is one of the goals of modeling SNe Ia. Obviously, the predictive power of self-consistent multi-dimensional SN Ia models is promising for progress in answering the questions arising from SN Ia cosmology.

In Sect. 2 we set out how the astrophysical scenario of SNe Ia is derived from observations. Numerical approaches to modeling SNe Ia are discussed in Sect. 3 with special emphasis on multi-dimensional models. As an illustrative example, a particular implementation of the deflagration SN Ia model is presented in Sect. 4, where also ways to test the validity of SN Ia models on the basis of comparison with observations are outlined and the application to questions arising from the cosmological

application of SNe Ia is discussed. Conclusions are drawn in Sect. 5.

2 Observations and astrophysical scenario

Observational features of SNe Ia suggest a specific astrophysical scenario. The cornerstones of the astrophysical model of SNe Ia are set by two fundamental characteristics of these events. Evidently, SNe Ia belong to the most energetic cosmic explosions, releasing about 10^{51} erg of energy. For a short period of time they can outshine an entire galaxy consisting of tens of billions of stars. SNe Ia spectra are characterized by the lack of indications for hydrogen and helium which together with a pronounced P Cygni silicon line at maximum light classifies these objects (Wheeler & Harkness, 1990). Lines of intermediate mass elements (such as Si, Ca, Mg and S) and oxygen are observed in near-maximum light spectra (e.g. Filippenko, 1997b,a). With respect to light curve and spectra observations SNe Ia form a class of remarkable homogeneity (e.g. Branch & Tammann, 1992).

Assuming supernovae to originate from single stellar objects, only their gravitational binding energy, released in a collapse towards a compact object (Zwicky, 1938), or its nuclear energy, released in explosive reactions (Hoyle & Fowler, 1960), come into consideration as possible energy sources. In the particular case of SNe Ia no compact object is found in the remnant excluding the first possibility. The homogeneity of the class of SNe Ia and the fact that no hydrogen is found in their spectra provides a strong hint that the object undergoing the nuclear explosion may be a white dwarf (WD) star consisting of carbon and oxygen (C+O).

Lightcurves of SNe Ia rise over a time scale of several days and decline over months. It is therefore clear that they cannot be powered directly by the explosion since the temperatures fall off much too rapidly in the expansion. This problem was solved by Truran et al. (1967) and Colgate & McKee (1969) who suggested that the ^{56}Ni produced in large amounts in the explosive thermonuclear burning provides the energy source for the optical event by radioactive decay to ^{56}Co and ^{56}Fe .

2.1 Progenitor evolution and ignition

A single WD is an inert object. How can it reach an explosive state? The only way to introduce the necessary dynamics into the system is to assume it to be part of a binary system and to gain matter from the companion. Several models have been proposed for this progenitor evolution.

In the *double degenerate* scenario (Iben & Tutukov, 1984; Webbink, 1984), two C+O WDs merge. The lighter of the two is disrupted and its matter accreted onto the heavier WD. To become a potential candidate for a SN Ia, the merger should eventually reach the Chandrasekhar-mass (i.e. of the maximum mass that is supported against gravitational collapse by the pressure of the degenerate electrons). Stellar evolution predicts that systems fulfilling this requirement should exist and indeed a potential candidate that will merge in less than one Hubble time has been detected (Napiwotzki et al., 2005). Mergers of two C+O WDs provide a natural explanation for the absence of hydrogen. However, numerical simulations indicate that the high

accretion rate onto the more massive WD leads to an off-center ignition and the subsequent burning could convert the material to oxygen, neon, and magnesium. A WD of this composition, however, tends to undergo a gravitational collapse rather than a thermonuclear explosion (e.g. Saio & Nomoto, 1985, 1998).

In the *single degenerate* scenario (Whelan & Iben, 1973; Nomoto, 1982; Iben & Tutukov, 1984), the WD accretes matter from a non-degenerate companion (either a main sequence or an AGB star). This idea was recently supported by the detection of the potential companion of Tycho Brahe's 1572 supernova (Ruiz-Lapuente et al., 2004), which is a solar-type star. A detailed analysis of this scenario, however, revealed that the accretion rates admissible here are restricted to a narrow window. Too low rates evoke nova eruptions in which the WD loses more material than accreted before and too high rates would lead to the formation of an extended He-rich envelope. Moderate accretion rates build up a degenerate He-shell which could detonate and trigger a detonation of the carbon-oxygen core. Since this happens before the WD reaches the Chandrasekhar-mass limit, such a SN Ia model is termed *sub-Chandrasekhar* explosion (Woosley & Weaver, 1994). Somewhat higher accretion rates, however, can lead to quiet hydrostatic burning of the accreted material processing it to carbon and oxygen. In this case, the WD may reach the Chandrasekhar mass (*Chandrasekhar-mass model*, Hoyle & Fowler, 1960; Arnett, 1969; Hansen & Wheeler, 1969). Potential candidates for such systems are Supersoft X-ray Sources (e.g. Kahabka & van den Heuvel, 1997). The limitation of the fuel available in the explosion to the Chandrasekhar mass ($\sim 1.4 M_{\odot}$) makes the described scenario particularly favorable since it provides a natural explanation for the striking uniformity of SNe Ia in the gross observational features. On the other hand, it is afflicted with great uncertainties. Achieving a stable mass transfer in the progenitor binary system to build up a Chandrasekhar mass WD is highly non-trivial (e.g. Nomoto & Iben, 1985) and the observational evidence for such systems is sparse.

Although the striking homogeneity holds for most SNe Ia (so-called Branch-normals, Branch et al., 1993), some events differ significantly. These explode much weaker (like SN 1991bg, see Filippenko et al. 1992a; Leibundgut et al. 1993) or more vigorous (like SN 1991T, see Phillips et al. 1992; Filippenko et al. 1992b; Ruiz-Lapuente et al. 1992; Jeffery et al. 1992; Spyromilio et al. 1992) than the average. At present it is unclear, whether the entire class of SNe Ia can be explained by only one progenitor scenario. The currently favored Chandrasekhar-mass model may possibly only be able to explain the Branch-normals while sub- and superluminous events require different progenitor scenarios. Therefore, even if currently not in the focus of research, the double-degenerate and the sub-Chandrasekhar mass scenarios may contribute to the SN Ia population. In the following, however, we will focus on the Chandrasekhar-mass model, since it received most attention in recent theoretical modeling.

When the WD approaches the Chandrasekhar limit, the density at the center of the WD increases rapidly so that fusion of carbon ignites. Contrary to the situation in main sequence stars, the degenerate material of the WD does not allow for moderation of the burning by expansion. Heat transport is achieved here by convection giving rise to a stage of convective carbon burning that lasts for several hundred years. This phase is terminated by one or more small spatial regions undergoing a thermonuclear runaway, marking the birth of a thermonuclear flame and the onset of the explosion. The convective burning stage and the conditions at flame ignition are extremely hard to model both analytically and numerically. Therefore the exact shape and location of the first flame spark(s) is not yet well constrained. These, however, are crucial initial parameters in multi-dimensional explosion models. Only a few studies addressed the flame ignition process so far. Garcia-Senz & Woosley (1995) simulated the thermonuclear runaway of a hot bubble floating upward from the center of the WD. They concluded that off-center and multi-spot ignitions are possible. A similar result was recently obtained by Iapichino et al. (2005). The convective phase directly preceding the ignition crucially influences the configuration of the initial flame. Here different studies led to controversial results. While Woosley et al. (2004) and Kuhlen et al. (2005) favor off-center, possibly multiple and asymmetrically distributed flame sparks, Höflich & Stein (2002) put forward a single central ignition.

2.2 Flame propagation and explosion

The goal of SN Ia explosion models is to follow the propagation of the thermonuclear flame from its ignition near the center of the WD outwards and to determine the composition and the distribution of the burning products in the ejected material.

Theoretically, SN Ia explosions are governed by the equations of reactive fluid dynamics, i.e. the Navier-Stokes equations extended with an equation of species balance, suitable terms for heat conduction, diffusion of species, and source terms of energy and species in combination with an equation of state (eg. Oran & Boris, 1987). These equations allow for solutions of traveling reaction waves converting unburnt to burnt material. If the scales under consideration are much larger than the internal structures of these waves, a simplified description of the system is possible. Neglecting all phenomena that actually govern the propagation of the reaction wave, i.e. the reaction kinetics and transport processes, the burning front is modeled as a moving discontinuity. This picture provides a description of the hydrodynamical state of the material in the unburnt and burnt regions and the equations simplify to the reactive Euler equations. From these, the Rankine-Hugoniot jump conditions for the state variables across the burning front follow (see Landau & Lifshitz, 1959) which allow for two different modes of front propagation. One is the subsonic deflagration in which the flame is mediated by the thermal conduction of the degenerate electron gas and the other is a supersonic detonation in which the burning front is driven by shock waves. Either one of these modes or a combination of both have been suggested in different explosion models.

- *The prompt detonation model* was first applied in a numerical simulation by Arnett (1969). A spherically symmetric detonation wave was initiated near the center of the WD and propagated outward. Criteria for the spontaneous formation of a detonation wave have been investigated by Blinnikov & Khokhlov (1986) and Woosley (1990). They reach the conclusion, that a detonation can initiate only under certain prerequisites. A prompt detonation as explosion model produces enough energy for a SN Ia event. However, ahead of a supersonic detonation wave the fuel cannot expand and is therefore incinerated at the high densities of an equilibrium white dwarf. This results in the almost complete conversion of the material to nickel-peaked nuclear statistical equilibrium (Arnett, 1969; Arnett et al., 1971), which is in conflict with the intermediate mass elements observed in SN Ia spectra. These nucleosynthetic problems rule out a pure detonation scenario as a standard model for SN Ia explosions.
- *The deflagration model* (Nomoto et al., 1976) assumes the flame propagating in the subsonic deflagration mode. The laminar burning speed of the deflagration flame is determined by microphysical transport processes. For conditions of carbon burning in C+O WDs it is highly subsonic (Timmes & Woosley, 1992) and therefore the flame propagates far too slowly to explain SN Ia explosions. The expansion of the star will quench burning before the WD gets unbound. On the other hand, this model can cure the problem of nucleosynthesis, since rarefaction waves travel ahead of the flame with sound speed and lower the fuel density prior to burning. Thus the material can partly be processed into intermediate mass elements.

The deflagration model undergoes a significant improvement when multidimensional effects are taken into account. The propagation of the deflagration front is subject to several instabilities (e.g. Niemeyer & Woosley, 1997). Of purely hydrodynamical origin is the Landau-Darrieus instability (Landau, 1944; Darrieus, 1938) which in the nonlinear stage is stabilized in a cellular pattern (Zel'dovich, 1966) thus enlarging the flame surface area and enhancing the net burning rate. The major effect accelerating the flame, however, is due to the buoyancy unstable flame propagation from the center of the star outwards. It leaves behind light and hot ashes below the dense fuel – a density stratification inverse to the gravitational acceleration. In its non-linear stage, the Rayleigh-Taylor instability leads to the formation of mushroom-shaped burning bubbles raising into the fuel. The Reynolds number typical for this situation is as high as 10^{14} . Clearly, shear (Kelvin-Helmholtz) instabilities at the interfaces of these bubbles will generate turbulent eddies which then decay to smaller scales forming a turbulent energy cascade. The flame will interact with these eddies down to the Gibson-scale at which the turbulent velocity fluctuations become comparable to the laminar flame speed. Below the Gibson scale, the flame burns faster through turbulent eddies than they can deform it, and the flame propagation is thus unaffected by turbulence there. This interaction corrugates the flame again increasing its surface and consequently accelerating the effective propagation speed.

- *The delayed detonation (DD) model* conjoins the advantages of the deflagration and the detonation models. It was put forward by Ivanova et al. (1974), Khokhlov (1991a), and Woosley & Weaver (1994). Burning starts out in the slow deflagration mode pre-expanding the star. Motivated by transitions from the deflagration to the supersonic detonation mode (deflagration-to-detonation transition, DDT) observed in terrestrial turbulent combustion processes, such a phenomenon is assumed to occur in SNe Ia. Its physical mechanism, however, remains unclear and therefore it enters the model as a free parameter. Usually, in one-dimensional (1D) simulations the DDT is artificially initiated once the flame reaches fuel of a certain transition density ρ_{tr} . The assumed detonation then burns the star until the flame is quenched by the expansion. This detonation is an easy way to explain the energy release necessary for a SN Ia explosion. The important notion in this model is that a detonation in low density fuel (pre-expanded in the deflagration stage) can lead to only partial burning and is therefore capable of generating intermediate mass elements. Another possible advantage of this model derives from a problem of current 3D implementations of the pure deflagration scenario. The Rayleigh-Taylor bubbles being the origin of the turbulent flame acceleration cause considerable amounts of unburnt C+O matter to remain in “fingers” near the center of the star, which are possibly in conflict with spectral SN Ia observations. A detonation wave initiated at later stages of the evolution could be capable to burning out those fingers and to process the previously unburnt material. The best agreement with observations was achieved for $\rho_{\text{tr}} \sim 1 \times 10^7 \text{ g cm}^{-3}$ (Höflich & Khokhlov, 1996; Iwamoto et al., 1999). The main disadvantage of the DD model is that this transition density remains an arbitrary parameter unless the mechanism of a possible DDT is physically determined (if there exists one at all, cf. Niemeyer, 1999).
- *The pulsational delayed detonation (PDD) model* (Arnett & Livne, 1994a,b) is similar to the DD model in the sense that it combines an initial deflagration with a later detonation. The flame is assumed to propagate in the initial deflagration phase with its laminar burning speed and pre-expands the star. Due to the slow flame velocity, the burning front stalls and fails to unbind the star. The WD then re-contracts giving the interface between burnt and unburnt material enough time to mix and to become nearly isothermal. Compressional heating finally triggers a detonation at densities that are lower than that prior to the first expansion phase. Höflich & Khokhlov (1996) employ this scenario in a phenomenological 1D model and conclude that it may account for sub-luminous SN Ia. However, the assumption that the flame propagates with the pure laminar burning velocity in the deflagration phase seems unrealistic, because of the flame instabilities and the resulting turbulent flame acceleration. Recent multidimensional deflagration models (Reinecke et al., 2002b; Gamezo et al., 2003) demonstrated that taking into account these effects, the star is likely to get unbound instead of recontracting.

3 Numerical models

3.1 Relevant scales

The numerical implementation of SN Ia models accounting for the full exploding WD star in multiple dimensions is significantly complicated by the wide range of relevant length scales involved in the problem. From the radius of the WD star (~ 2000 km at the onset of the explosion and expanding in the process) it reaches down to the flame width which is well below one centimeter. In the deflagration model the relevance of turbulent effects amplifies the scale problem since the turbulent cascade extends to the even much smaller Kolmogorov scale where the turbulent energy is dissipated into heat. Here, the flame interaction with the turbulent cascade down to the Gibson scale must additionally be taken into account. Current 3D simulations capturing the entire star reach resolutions around one kilometer while the Gibson scale is of the order of 10^4 cm at the beginning of the explosion and decreases steadily.

For large-scale multi-dimensional SN Ia simulations this has three consequences.

1. The internal flame structure cannot be resolved. Thus, an effective flame model has to be applied and complementary small scale simulations are required.
2. It is not possible to fully resolve the interaction of the flame with turbulence. Therefore modeling of the effects on unresolved scales is necessary.
3. Assumptions about the flame properties at unresolved scales (e.g. stability below the Gibson scale) have to be validated in separate small-scale simulations.

3.2 Modeling approaches

Numerical models of SN Ia explosions have to face three major challenges. Apart from the vast range of relevant length scales they need to take into account inherently three-dimensional physical phenomena and to solve the kinetics of nuclear burning. To meet all these requirements in a single simulation will be impossible in the foreseeable future. Therefore the problem has been tackled in different approaches.

The first path towards SN Ia explosion modeling is to restrict the simulations to only one spatial dimension. Here, in principle a resolution of the relevant scales is achievable and a detailed description of the nuclear reactions is feasible. However, crucial three-dimensional physical mechanisms are not explicitly taken into account and need to be parametrized. Although such models were shown to yield good fits to observations and pioneered the insight into fundamentals of the explosion process, they lack consistency and are of little predictive power.

In multi-dimensional simulations, contrariwise, the computational costs of modeling the explosion hydrodynamics is prohibitive to directly resolve all relevant scales as well as details of the nuclear processes. While the latter may be improved in the forthcoming years, and is meanwhile separated from the actual explosion simulations still maintaining a reasonable accuracy (see below), even a drastic increase in computational capabilities will not allow for a resolution of all scales in multi-dimensional simulations.

A third approach is to study specific effects on a limited range of spatial scales, to validate assumptions and improve modeling techniques of the large-scale SN Ia simulations.

3.3 One-dimensional simulations

Although we focus on multi-dimensional models of SN Ia explosions, we will first give a brief overview of 1D spherically symmetric simulations. Since (at least in the initial deflagration stage) the propagation velocity of the thermonuclear flame is determined by multi-dimensional effects, such as instabilities and interaction with turbulent velocity fluctuations, a physically undetermined speed is ascribed to the spherical burning front. This free parameter can be used to fit the observations and therefore give a hint to the expected average temporal evolution of the flame in multi-dimensional simulations. The best known of these models, W7, was presented by Nomoto et al. (1984) and Thielemann et al. (1986) and has been employed in several studies since then (e.g. Iwamoto et al., 1999; Brachwitz et al., 2000). Here the flame propagation speed was modeled with mixing length theory and started slowly to pre-expand the star. Later it strongly accelerated and consumed large fractions of the star converting the material to iron-group elements (mainly ^{56}Ni) and intermediate mass elements. Different ways to parameterize the flame propagation velocity were proposed by Nomoto et al. (1976), Woosley (1990), Höflich & Khokhlov (1996), and Niemeyer & Woosley (1997). All these models conclude that a flame acceleration to one third of the sound speed is necessary for consistency of the results with observations. The problem of overproduction of neutron-rich iron-group material noted in these models may be significantly reduced when taking into account revised electron capture rates (Brachwitz et al., 2000).

When applying 1D models to simulate delayed-detonation scenarios, the condition for the DDT comes into play as a second undetermined parameter. Such models are capable of providing excellent fits to lightcurves and spectra and seem to yield reasonable compositions of the nucleosynthesis products (Woosley, 1990; Höflich & Khokhlov, 1996; Khokhlov, 1991b; Iwamoto et al., 1999).

Although lacking consistency and therefore predictive power, 1D models have been employed to address questions arising from SN Ia cosmology, such as the origin of the diversity in these objects (Bravo et al., 1993, 1996; Höflich & Khokhlov, 1996; Höflich et al., 1998; Umeda et al., 1999; Iwamoto et al., 1999; Domínguez & Höflich, 2000; Domínguez et al., 2000, 2001).

3.4 Multi-dimensional simulations

Initiated by Müller & Arnett (1982, 1986), multi-dimensional models were applied to fix the turbulent flame propagation velocity undetermined in spherically symmetric simulations. Given the wide range of scales on which the flame is affected by turbulence, this is an ambitious project, additionally challenged by the lack of resolution of the thermonuclear flame structure. For both problems, different approaches have been taken. All these were guided by the theory of turbulent combustion in terrestrial flames (see Peters, 2000).

3.4.1 Hydrodynamics

The hydrodynamical equations are discretized either in a Lagrangean or Eulerian approach. The Smooth Particle Hydrodynamics (SPH) technique used by Garcia-Senz et al. (1998) falls into the first category, while an implicit scheme on an Eulerian grid is applied by Livne (1993). Most explicit Eulerian approaches were based on versions of the PROMETHEUS implementation (Fryxell et al., 1989) of the Piecewise Parabolic Method (PPM) proposed by Colella & Woodward (1984). These include the simulations of Arnett & Livne (1994a,b), Khokhlov (1995), Niemeyer & Hillebrandt (1995b); Niemeyer et al. (1996), Reinecke et al. (1999a), Hillebrandt et al. (2000), Reinecke et al. (2002b), Gamezo et al. (2003, 2004), Röpke & Hillebrandt (2004), Calder et al. (2004), Plewa et al. (2004), Röpke (2005), Röpke & Hillebrandt (2005a,b), Röpke et al. (2005a, 2006a) and Gamezo et al. (2005). An alternative approach was taken by Bell et al. (2004a), who modified the hydrodynamical equations to account for low-Mach number flows only. This provides an efficient scheme to numerically simulate subsonic deflagrations.

The facts that the WD star is expanding and that the flame is not necessary domain-filling in all stages of the explosion is taken into account in the grid-based schemes in various approaches. While Reinecke et al. (1999a, 2002b) use a static computational grid with a fine-resolved central part and a coarse outer grid to account for the expansion, Röpke (2005) implemented a uniform moving grid that co-expands with the exploding WD. Since on average the explosion process is more or less spherical, one can gain resolution in the part of the star occupied by the flame with nested moving grids (Röpke et al., 2006a). A different technique providing resolution where needed is adaptive mesh refinement as applied in the simulations by Gamezo et al. (2003) and Calder et al. (2004).

3.4.2 Flame model

In earlier works (Müller & Arnett, 1986; Livne, 1993) the flame was advanced according to discrete boolean criteria. A computational cell was burned if certain conditions in neighboring cells were fulfilled. This strategy is clearly dependent on the grid geometry and therefore in recent simulations different approaches have been taken. Two major strategies to tackle the problem of the unresolved internal flame structure can be distinguished. Khokhlov (1993, 1994, 1995) adapted a flame capturing technique that mimics flame propagation by an artificial diffusion mechanism which broadens the internal flame structure to a certain number of computational grid cells. This method was applied in the SN Ia explosion simulations by Gamezo et al. (2003, 2004, 2005), Calder et al. (2004), and Plewa et al. (2004). A completely different approach was taken by Reinecke et al. (1999b), who treat the flame as a sharp discontinuity separating the fuel from the ashes. It is numerically represented applying the level-set technique (Osher & Sethian, 1988; Sethian, 1996). Here the flame front is associated with the zero level set of a scalar function G representing the distance from the interface. A model for flame propagation based on this technique was developed by Smiljanovski et al. (1997) and a modified version for thermonuclear flames in SN Ia explosion was presented by Reinecke et al.

(1999b) (for details of the implementation see also Hillebrandt et al., 2005). This scheme was applied in the simulations by Hillebrandt et al. (2000), Reinecke et al. (2002c,a,b), Röpke & Hillebrandt (2004, 2005b,a), Röpke (2005), Schmidt et al. (2005c), Schmidt & Niemeyer (2006), and Röpke et al. (2005a, 2006a).

3.4.3 Turbulent combustion model

As outlined above, SN Ia explosions are believed to at least start out subsonically in the deflagration mode of flame propagation. Thus the flame is subject to the interaction with turbulence generated by instabilities. This mechanism turns out to be crucial to accelerate the flame propagation and must therefore be taken into account in any valid SN Ia model.

The theory of turbulent combustion has been extensively developed for terrestrial combustion phenomena (see Peters, 2000). The nuclear reaction kinetics in thermonuclear combustion waves is much simpler than the chemical reactions in terrestrial flames and due to the high thermal conductivity of the degenerate electron gas in WD matter some of the characteristic nondimensional numbers differ. Nonetheless, the turbulent combustion process in the deflagration mode in SNe Ia bears striking similarity to *premixed turbulent flames* (i.e. turbulent flames in mixtures of fuel and oxidizer) in terrestrial combustion processes.

The wide range of scales involved in turbulent combustion phenomena renders direct simulations impossible for most situations. Therefore only parts of the interaction range of the flame with turbulence and the resulting surface enlargement of the flame can be resolved. This is usually compensated by attributing an effective *turbulent flame speed* s_t to the unresolved flame front, which must be determined by theoretical considerations. One of the cornerstones of the theoretical description of turbulent combustion is the notion of different regimes of flame/turbulence interaction (Niemeyer & Kerstein, 1997). These regimes are distinguished by the ability of turbulent eddies to penetrate the internal flame structure. Since the Gibson scale is much larger than the flame width for most parts of the SN Ia explosion, this will not be the case here and accordingly the combustion falls into the regime of *wrinkled and corrugated flamelets*. Here, the full flame structure is corrugated by the interaction with turbulence and the resulting surface enlargement accelerates its propagation. As first noted by Damköhler (1940), the flame propagation in this regime completely decouples from the microphysics of the burning for sufficiently strong turbulence. It is entirely determined by the turbulent velocity fluctuations, that is, s_t is proportional to the turbulent velocity fluctuations.

One of the challenges of deflagration models of SN Ia explosions is thus to determine these velocity fluctuations correctly. Since the resolution in multi-dimensional simulations is insufficient to resolve the phenomena directly, modeling approaches have to be taken. In the simplest models, a minimal propagation velocity of the flame is artificially imposed, which is not physically determined in the model (García-Senz & Bravo, 2005). Contrary to this, Gamezo et al. (2003), and Calder et al. (2004) assume the flame to be driven by buoyancy-induced instabilities on unresolved scales giving rise to a turbulent flame speed of $s_t = 0.5 \sqrt{Ag_l}$, where g and l denote the gravitational acceleration and the computational grid cell size, re-

spectively. A is the Atwood number derived from the density contrast over the flame front. A more sophisticated approach was proposed by Niemeyer & Hillebrandt (1995a). Guided by the technique of *Large Eddy Simulations* they implemented a turbulent subgrid-scale model (Clement, 1993) in SN Ia explosion simulations. This model determines the turbulence energy on unresolved scales based on conservation laws. The hyperbolic nature of the equations of hydrodynamics, however, does not allow for a closed system of equations here so that closure assumptions have to be invoked. A physically better motivated approach based on localized closures was recently proposed by Schmidt et al. (2005b,c).

In the very late stages of the SN Ia explosion the fuel density drops due to expansion of the WD to values where the flame width becomes broader than the Gibson length. Then, turbulence penetrates the internal structure of the flame and it enters the regime of *distributed burning* (Niemeyer & Kerstein, 1997). Here, different scaling laws for the turbulent flame speed apply (Damköhler, 1940) and a preliminary test of the effects on SN Ia models was given by Röpke & Hillebrandt (2005b).

3.4.4 Nuclear reactions

The computational expenses for a full nuclear reaction network are prohibitive to run it concurrently with the explosion hydrodynamics simulations in present multi-dimensional models. Since here the only dynamically relevant parameter is the energy release in the reactions, it is sufficient to apply a simplified description. Usually, only a few nuclei representative for the fuel mixture, the iron group elements and the intermediate mass elements in the ashes and effective reactions between them are accounted for (e.g. Reinecke et al., 2002a).

However, in order to derive observables (such as lightcurves and spectra) from the explosion models, the exact chemical composition of the ejecta needs to be known. This can be achieved by advecting a number of tracer particles in the explosion hydrodynamics simulations which record the evolution of temperature and density. This adds a Lagrangean component to the Eulerian code. Based on the data gained from the tracer particles it is then possible to *a posteriori* reconstruct the detailed nuclear reactions in the burnt material with extended nuclear reaction networks. This technique was implemented for SNe Ia by Travaglio et al. (2004) and also applied in the study by Röpke et al. (2005a).

3.4.5 Results of multi-dimensional models

While earlier two-dimensional (2D) deflagration models of SN Ia failed to explode (e.g. Khokhlov, 1995) others succeeded to (weakly) unbind the WD Niemeyer et al. (1996). Nowadays, it seems that a consensus has been reached on the general capability of the 3D version of this model to give rise to robust explosions (Reinecke et al., 2002b; Gamezo et al., 2003; Röpke & Hillebrandt, 2005a). Although the energetics (asymptotic kinetic energy up to 7×10^{50} erg) and the production of ^{56}Ni ($\sim 0.4 M_{\odot}$) as the main global characteristics fall into the range of observational expectations (Contardo et al., 2000; Stritzinger et al., 2005), they are still on the weaker side of “normal” SNe Ia.

Since the initial flame configuration in the explosion is undetermined yet (see Sect. 2.1), several studies addressed its effect on the outcome of the simulations. Off-center ignitions were analyzed based on 2D-simulations by Niemeyer et al. (1996) and 3D-full star simulations by Calder et al. (2004). The latter study indicated that a single perfectly spherical off-center initial flame quickly emerges to the surface of the WD and fails to burn sufficient material to explode it. Plewa et al. (2004) suggested that the material breaking through the surface of the still gravitationally bound WD may collimate on the opposite side of it, evoking a detonation there. Contrary to that, Röpke & Hillebrandt (2005a) found that a more structured off-center initial flame (motivated by pre-ignition convection, cf. Sect. 2.1) stays more or less in place and gives rise to a viable explosion. The effects of the number of ignition spots have been addressed in several 2D studies (Niemeyer et al., 1996; Reinecke et al., 1999a; Livne et al., 2005) giving a wide range of results dependent on the number and distribution of the initial flame kernels and in 3D simulations (Reinecke et al., 2002b; Röpke & Hillebrandt, 2005a; Röpke et al., 2006a; García-Senz & Bravo, 2005). These simulations indicate that multi-spot ignition scenarios can lead to more vigorous explosions than centrally ignited setups and put the deflagration scenario in better agreement with observations. Interestingly, the 3D simulations, although also exhibiting a dependence on the number of ignition spots, gave much more robust results than the 2D studies (Röpke et al., 2006a). Similar conclusions were drawn on the basis of a stochastic ignition model in which a spatial and temporal distribution of the flame ignition spots was assumed (Schmidt & Niemeyer, 2006).

A successful explosion, however, is not the only requirement for a valid SN Ia model. Observables derived from such models must match the observations of SNe Ia. Moreover, the model must allow for a certain variation of the results in order to reproduce the observed range of diversity in the characteristics. No general consensus has been reached so far regarding these questions. Besides the low explosion energies and ^{56}Ni production the problems of most deflagration simulations include unburnt material left behind at low velocities in the ejecta due to downdrafts in the buoyancy-induced large-scale flame pattern and low production of intermediate mass elements. Recently, a series of 3D simulations was analyzed to determine whether these shortcomings are generic to the deflagration model or caused by the simplicity of some setups. It seems that the model is generally capable of reproducing main observational features, but some of the problems persist (see Sect. 4 for details).

Gamezo et al. (2004) claim that a delayed detonation is necessary to achieve agreement with observations. In their 3D model, a detonation front is artificially initiated after a deflagration stage at a pre-selected time and location. As expected, it travels through the WD burning most of the material in the inner parts. A 2D implementation of the delayed detonation model was recently presented by Golombek & Niemeyer (2005). Here, the DDT is assumed to occur when the deflagration flame enters the distributed burning regime which apparently happens first in the outer parts of the flame front. This rises the question of whether the detonation (if not allowed to travel through ashes) can catch up with the expanding material on the opposite side of the WD. 2D simulations by Steinmetz et al. (1992) studied

pure prompt detonation in rapidly rotating WDs. Although here regions may exist with densities allowing for the production of intermediate mass elements, the authors conclude, that the ratio of iron group elements to intermediate mass elements arising from such models is inconsistent with normal SNe Ia.

To settle the question of the explosion mechanism, detailed analysis of the different models and comparison with observations on the basis of synthetic light curves and spectra are required.

3.5 Complementary small-scale simulations

Complementary studies of flame propagation on small scales focus on effects in only a narrow window in scale space. These therefore reach a much higher resolution and can model the processes in a more realistic way than SN Ia simulations on scales of the WD star. Consequently, they give insight into mechanisms that are unresolved there either testing the validity of assumptions or providing input data to these models.

On the basis of resolved 1D flame simulations, Timmes & Woosley (1992) determined the laminar speed of deflagration flames in SNe Ia and Sharpe (1999) analyzed the propagation velocity of detonations. Both serve as input in multi-dimensional simulations (Reinecke et al., 2002b; Golombek & Niemeyer, 2005).

Other studies concerned the validity of subgrid-scale models of the interaction of the flame with turbulence (Schmidt et al., 2005a). This interaction was also simulated by Niemeyer et al. (1999). The deflagration flame propagation on small scales in SNe Ia subject to the Rayleigh-Taylor instability was tested in 2D-simulations by Khokhlov (1993) and Bell et al. (2004c) and in 3D-setups by Khokhlov (1995) and Zingale et al. (2005). The effects of the Landau-Darrieus instability on the thermonuclear flame have been analyzed in 2D-simulations by Niemeyer & Hillebrandt (1995a), Blinnikov & Sasorov (1996), Röpke et al. (2003), Röpke et al. (2004a,b), and Bell et al. (2004b). Dursi et al. (2003) studied the response of thermonuclear flame to curvature and stretch. Most of these simulations confirm the assumptions made in large-scale SN Ia models.

The question whether a transition of the turbulent burning regime from flamelet to distributed burning would cause a deflagration-to-detonation transition was addressed by Lisewski et al. (2000b,a), who conclude that such an event is very unlikely.

4 Example: A deflagration SN Ia model

To illustrate the numerical modeling of SN Ia explosions in three spatial dimensions, a deflagration model in a specific implementation shall be discussed in this section. It starts out with a cold isothermal ($T = 5 \times 10^5$ K) Chandrasekhar-mass WD. Unless otherwise stated, its composition was assumed to consist of equal parts of carbon and oxygen.

4.1 Numerical techniques

The numerical techniques forming the foundation of the implementation of the deflagration SN Ia model presented here are described by Reinecke et al. (1999b), Röpke (2005), Schmidt et al. (2005b), and Niemeyer & Hillebrandt (1995b). The fundamental approach is that of *Large Eddy Simulations*, where hydrodynamics on the resolved scales is modeled in a *finite volume approach* based on the PROMETHEUS implementation (Fryxell et al., 1989).

The equation of state describing WD material contains contributions from an arbitrarily degenerate and relativistic electron gas, an ideal gas of nuclei, radiation, and possibly electron-positron pair creation and annihilation.

As a consequence of 2 of the enumeration in Sect. 3.1, a *subgrid-scale model* is applied to account for turbulent effects on unresolved scales. Some older simulations follow the implementation suggested by Niemeyer & Hillebrandt (1995b), while one recent highly resolved run applied the updated modeling approach of Schmidt et al. (2005b).

According to 1 of the enumeration, the flame representation is achieved in a modeling approach. Seen from the scales of the WD star, the flame appears as a sharp discontinuity separating the fuel from the ashes. A suitable numerical method to follow the evolution of such an interface is the *level set technique* introduced to SN Ia modeling by Reinecke et al. (1999a). In this implementation, the flame propagation speed needs to be prescribed. This quantity, however, is not arbitrary in the presented modeling framework. For turbulent combustion in the flamelet regime (cf. Sect. 3.4.3), which applies to the burning in major parts of SN Ia explosions, it is given by the turbulent velocity fluctuations. These are determined by the subgrid-scale turbulence model.

Nuclear reactions are implemented in the simplified approach (cf. Sect. 3.4.4) proposed by Reinecke et al. (2002a). The progenitor material is composed of ^{12}C and ^{16}O . At high fuel densities nuclear burning terminates in nuclear statistical equilibrium represented by a mixture of ^{56}Ni and α -particles. Once the fuel density drops below $5.25 \times 10^7 \text{ g cm}^{-3}$, burning will become incomplete and intermediate mass elements (represented by ^{24}Mg) are produced. The respective difference in nuclear binding energy is released which provides sufficient accuracy to model the dynamics of the explosion. The chemical composition of the ejecta is derived in a postprocessing step (Travaglio et al., 2004).

4.2 Results of Simulations

Several simulations based on the implementation described above, both in two and three spatial dimensions, have been presented by Reinecke et al. (1999a, 2002a,b). In the 2D simulations, numerical convergence in the global quantities was demonstrated. For the implementation on a co-expanding computational grid, a similar result was found by Röpke (2005) (see Fig. 1). The numerical convergence naturally arises from the interplay of the resolved flame front representation with the turbulent subgrid-scale model. Ideally, a lack of resolution of large-scale features in the flame front representation should be compensated by an increased turbulent flame prop-

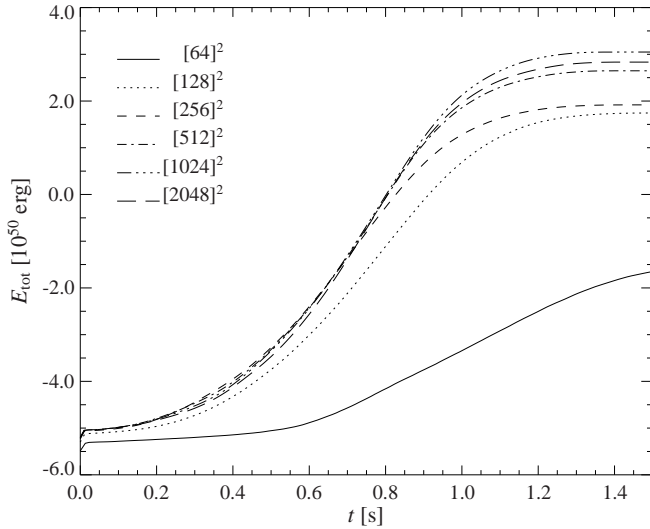


Figure 1: Total energy in 2D-simulations with co-expanding grid for different numbers of computational grid cells.

agation velocity determined from the subgrid-scale approach. Of course, a certain threshold of resolution will need to be exceeded to reach this regime in the numerical implementation.

One requirement to reliably derive observables from simulations is that the evolution of the models be followed to the stage of homologous expansion. In this hydrodynamically relaxed situation, the velocity of the ejected material is proportional to its radius. Obviously, a static computational grid that sufficiently resolves the flame propagation does not allow to follow the expansion over sufficiently long time scales. Therefore Röpke (2005) proposed to use a moving computational grid that co-expands with the WD. With this implementation it is in principle possible to follow the evolution for arbitrary times, but (Röpke, 2005) showed that simulating the first 10 s after ignition is sufficient to reach homology with reasonable accuracy. An example of such a simulation is shown in Fig. 2, where the isosurface represents the zero level set of G and is associated with the flame front. This simulation was carried out on only one octant of the WD assuming mirror symmetry to the other octants. The flame was ignited centrally with a toroidal perturbation superposed to the spherical shape. Of course, at times after ~ 2 s when burning terminates in the model, the zero level set of G loses physical meaning, but it still indicates the approximate boundary between unburnt material and ashes.

Due to the high computational expenses, most 3D simulations (such as the one described above) comprise only one octant of the WD. However, only full-star setups allow to account for asymmetry effects. On the basis of spectropolarimetry observations of several SNe Ia (e.g. Wang et al., 2003) these are expected to occur in at least some explosions. Röpke & Hillebrandt (2005a) showed, that in the deflagration

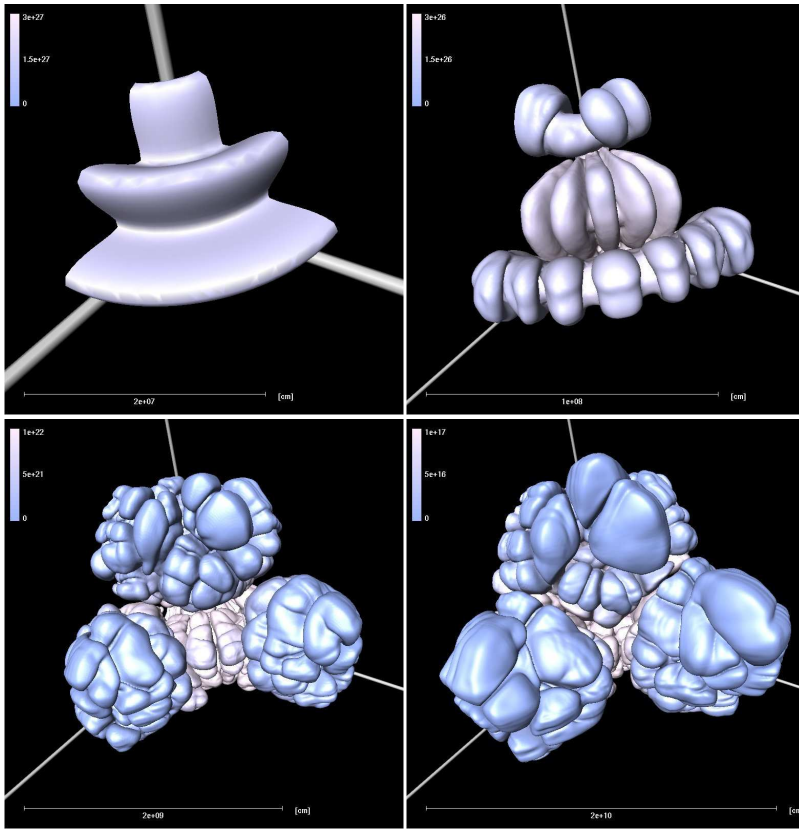


Figure 2: Snapshots from a single-octant SN Ia simulation performed on a uniform expanding computational grid. The isosurface corresponds to $G = 0$ and is color-coded with a measure of the turbulence strength derived from the subgrid-scale model (top left to bottom right: ignition flame, 0.5 s, 2.0 s, and 10.0 s after ignition).

model such asymmetries arise exclusively from irregularities in the flame ignition conditions and not from large-scale instabilities and resulting preferred modes in the flow patterns. Therefore, fixing a symmetric initial flame shape and studying the influence of other physical parameters on single-octant explosion models is a valid approach (see Sect. 4.4 below).

To illustrate the typical flame evolution in deflagration SN Ia models, the full-star model presented by Röpke & Hillebrandt (2005a) shall be described here. It started out from an asymmetric initial flame configuration which was set up by randomly distributing spherical flame kernels around the center of the WD. This resulted in a foamy structure slightly misaligned with the center of the WD.

Starting from this initial flame configuration (shown in Fig. 3), the evolution of the flame front in the explosion process is illustrated by snapshots of the $G = 0$ isosurface at $t = 0.3$ s and $t = 0.6$ s in Fig. 3. The development of the flame shape from

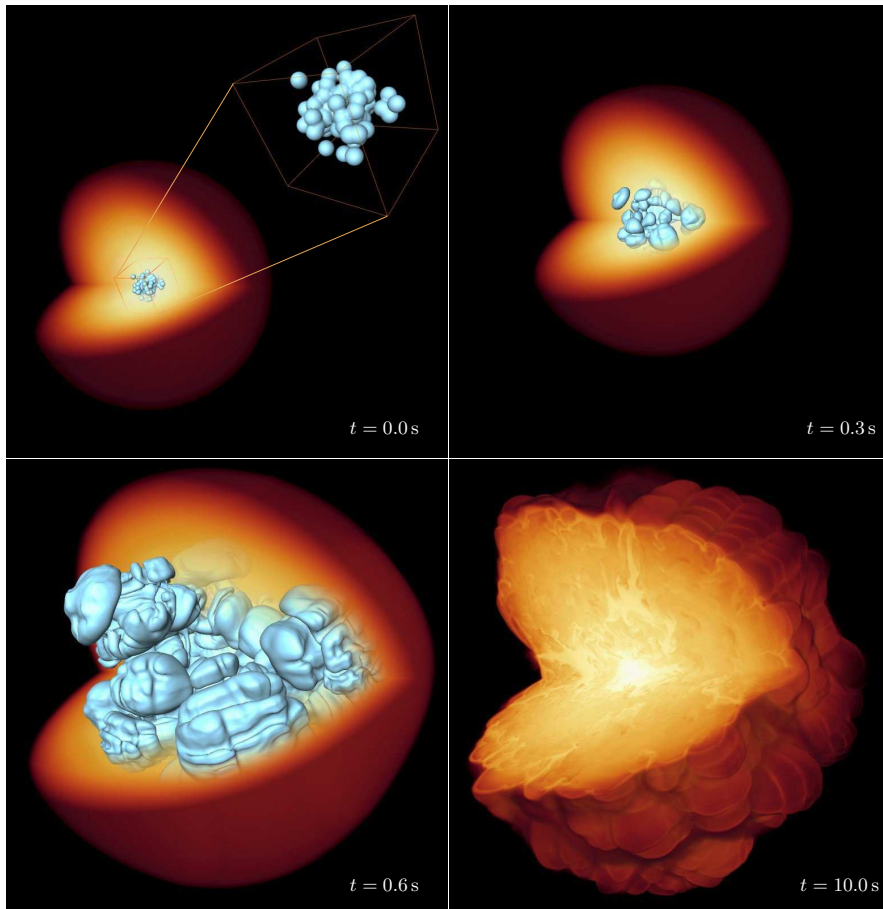


Figure 3: Snapshots from a full-star SN Ia simulation starting from a multi-spot ignition scenario. The logarithm of the density is volume rendered indicating the extend of the WD star and the isosurface corresponds to the thermonuclear flame. The last snapshot corresponds to the end of the simulation and is not on scale with the earlier snapshots.

ignition to $t = 0.3$ s is characterized by the formation of the well-known “mushroom-like” structures resulting from buoyancy. This is especially well visible for the bubbles that were detached from the bulk of the initial flame. But also the perturbed parts of the contiguous flame closer to the center develop nonlinear Rayleigh-Taylor like features. During the following flame evolution, inner structures of smaller scales catch up with the outer “mushrooms” and the initially separated structures merge forming a more closed configuration (see snapshot at $t = 0.6$ s of Fig. 3). This is a result of the large-scale flame advection in the turbulent flow and the expansion of the ashes. Up to this stage the flame was strongly anisotropic. However, in the

later evolution a preferentially lateral growth of bubbles filled with ashes smoothes out parts of the anisotropies. The flame develops a more spherical shape and only a slight anisotropy is retained. After about 2 s self-propagation of the flame due to burning has terminated in the model. The subsequent evolution is characterized by the approach to homologous expansion. The resulting density structure at the end of the simulation is shown in the $t = 10$ s snapshot of Fig. 3. The flame evolution agrees with the expectations outlined in Sect. 2.2.

Since the flame ignition process is not modeled in the explosion simulations, there exists considerable freedom in choosing the number and distribution of ignition kernels (cf. Sect. 2.1). The results from models starting with a central ignition (cf. Fig. 2) indicate that such a setup leads only to weak explosions. Recently, the capabilities of multi-spot ignition models have been analyzed in a systematic way. This was possible due to a modification of the moving grid implementation to two nested grids. An inner, fine-resolved grid follows the flame propagation while an outer coarse grid tracks the WD expansion (Röpke et al., 2006a). In this way, it is possible to accumulate a large fraction of the available computational cells in the inner regions thereby resolving detailed multi-ignition configurations. Confining the ignition volume around the center of the WD, it may be expected that there exists a certain number of ignition spots which maximizes the burning and energy release. A sparse ignition would decrease the flame surface and thus the burning rate, while a too dense distribution of flame kernels will lead to a rapid merging of flame parts again decreasing the surface area. This was confirmed by the simulations, which however did not sharply single out an optimal number of ignition points but revealed a rather robust behavior over a wide range. Extreme cases, however, reproduced the anticipated dependence.

4.3 Comparison with observations

Due to recent progress in deriving observables from multi-dimensional deflagration simulations, a direct comparison with details of observations of nearby SNe Ia has come into reach. Since these contain no other parameters than the initial conditions, the question arises if the outcome of simulations as the ones described above meets the observational constraints. Such constraints result from the global characteristics derived from observations, observed light curves, and spectra taken from nearby SNe Ia.

The global characteristics derived from SN Ia observations state that a valid explosion model should release around 10^{51} erg of energy and produce $\sim 0.4 \dots 0.7 M_{\odot}$ of ^{56}Ni in the nuclear burning (Contardo et al., 2000; Stritzinger et al., 2005). However, there exists a large diversity in the observations ranging from the class of sub-luminous SNe Ia (like SN 1991bg with probably $\sim 0.1 M_{\odot}$ of ^{56}Ni) to super-luminous events (e.g. SN 1991T with a ^{56}Ni mass close to $1 M_{\odot}$). Deflagration models started with a multi-spot ignition setup typically possess $6 \dots 8 \times 10^{50}$ erg of asymptotic kinetic energy of the ejecta. They produce up to $\sim 0.4 M_{\odot}$ of ^{56}Ni . Thus they fall into the range of observational expectations, but in the current stage do not account for the more energetic SNe Ia. One reason for the low energetics may be that in the presented implementation nuclear burning is assumed to cease when

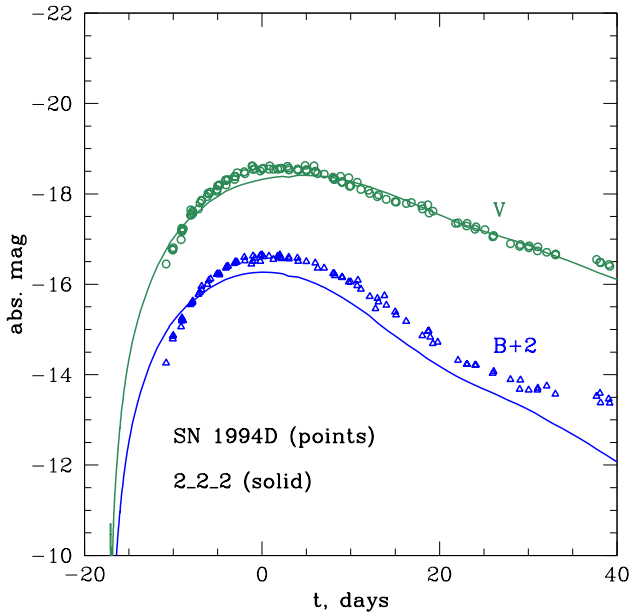


Figure 4: Synthetic light curves derived from model 2_2_2 of (Röpke et al., 2005a) (solid curves) compared with observed light curves from SN 1994D.

the fuel density drops below 10^7 g cm^{-3} , because the flame is then expected to enter the distributed burning regime. An approach to handling this stage was given by Röpke & Hillebrandt (2005b).

4.3.1 Lightcurves

A further requirement is that synthetic lightcurves agree with observed ones. These are sensitive to the energy release, the ^{56}Ni production, as well as to the distribution of elements in the ejecta. In Fig. 4 synthetic light curves derived from the 2_2_2 simulation (Röpke et al., 2005a) are compared with observations of SN 1994D¹ (Blinnikov et al., 2005, see also Sorokina & Blinnikov, 2003). The multi-band light curve of this model was calculated using the STELLA code of Blinnikov et al. (1998) and Blinnikov & Sorokina (2000).

The model produced $0.3 M_{\odot}$ of ^{56}Ni , although observations require somewhat higher ^{56}Ni mass ($\sim 0.4 M_{\odot}$) for the assumed distance. Nonetheless, there is generally very good agreement in the B and V bands near peak luminosities and in decline rate 20 days after the peak which is most important for cosmological applications of type Ia supernovae.

¹The distance to SN 1994D is still controversial and here the value of 30.4 is adopted from Drenkhahn & Richtler (1999)

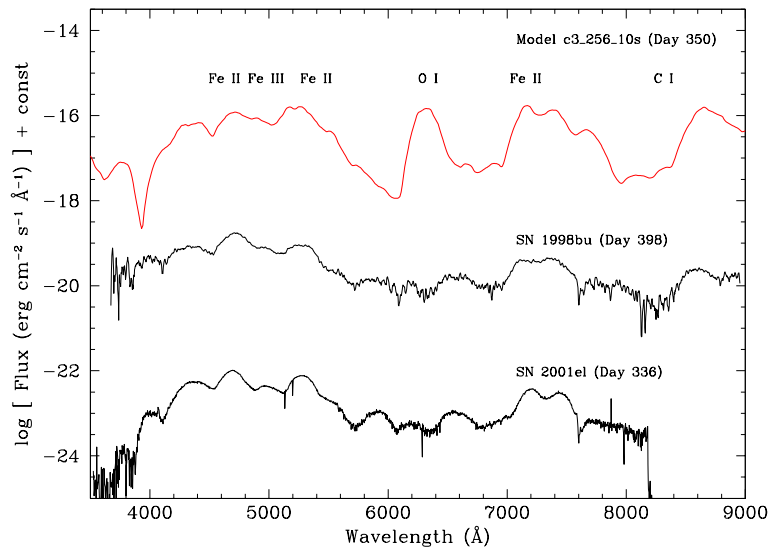


Figure 5: Synthetic nebular spectrum compared with observations (from Kozma et al., 2005).

4.3.2 Spectra

A much harder test for the models is posed by the comparison of synthetic with observed spectra since these depend on details in the composition of the ejected material.

Nebular spectra provide a means of studying the central parts of the ejecta, since they are taken at epochs where these have become transparent due to expansion. Thus they explore the “heart of the explosion” and are a valuable tool to study details of the physical processes involved in the explosion stage. Unfortunately, only one single synthetic late time spectrum is available from deflagration SN Ia models (Kozma et al., 2005). It was derived from the simulation shown in Fig. 2. The artificial and simple initial flame shape chosen here gives reason to not expect a good agreement between model and observation. However, as shown in Fig. 5, the broad iron features of the observed spectra are qualitatively reproduced. An inconsistency of the model with the observed nebular spectra is the appearance of a pronounced oxygen line at 6300 \AA . Both features of the synthetic spectrum share a common origin. The broad iron lines are caused by NSE material that is transported in the uprising plumes of ashes and thus distributed in velocity space. At the same time strong downdrafts carry unburnt material towards the center of the WD.

The disagreement may in part be attributed to the simplicity of the explosion model. Its highly symmetric initial flame shape with large imprinted perturbations favors a pronounced evolution of large-scale Rayleigh-Taylor features. This problem, however, is not necessarily generic to all SN Ia deflagration models. Multi-spot ignitions may lead to a more complete burning in the central parts of the WD. This

Table 1: Variation of initial parameters in SN Ia explosion models.

Parameter	range of variation	effect on ^{56}Ni production	effect on total energy
$X(^{12}\text{C})$	[0.30,0.62]	$\leq 2\%$	$\sim 14\%$
ρ_c [10^9 g/cm 3]	[1.0,2.6]	$\sim 6\%$	$\sim 17\%$
Z [Z_\odot]	[0.5,3.0]	$\sim 20\%$	none

was demonstrated by Röpke et al. (2006a). For an optimal number of ignition bubbles (and a rather wide range around this number), the central parts of the ejecta become dominated by iron group elements. Whether the achievable suppression of unburnt material at low velocities is sufficient to be consistent with observations needs further study.

A powerful diagnostic tool to compare SN Ia models with observations is provided by the abundance tomography presented by Stehle et al. (2005). It makes use of spectra taken from SN 2002bo with an extraordinary good time coverage. Fitting this sequence of data with synthetic spectra unveils the composition of the ejecta in velocity space slice by slice, since the photosphere moves gradually inwards with the expansion of the remnant. This abundance tomography of the ejecta can be compared with results of 3D models, when averaged over the angles. Qualitatively, the mixed composition of the ejecta found by Stehle et al. (2005) is reproduced by deflagration SN Ia models in a natural way since these predict a distribution of burnt material with the rising bubbles. A problem was, however, that older predicted large unburnt material fractions in the central parts of the ejecta in disagreement with the results of Stehle et al. (2005). A recent high-resolved simulation cures this problem by clearly reproducing the iron-group dominance in the low-velocity ejecta (Röpke et al., 2006b).

4.4 Diversity and correlations

The recent developments in the deflagration SN Ia explosion modeling outlined in the previous section seem to indicate that such a model is capable of reproducing the main features of observed objects but they do not rule out the alternative of a delayed detonation.

Here, the question of how multi-dimensional SN Ia models can be applied to tackle questions from the cosmological applications of these objects shall be illustrated on a set of simple deflagration models. Of particular interest is how such models behave under variation of physical parameters. Do they reproduce the observed diversity of SNe Ia? Are correlations between observables evident in the results?

Unfortunately, 3D deflagration models of SNe Ia as described above are computationally expensive. To moderate these expenses, simplified setups may be used

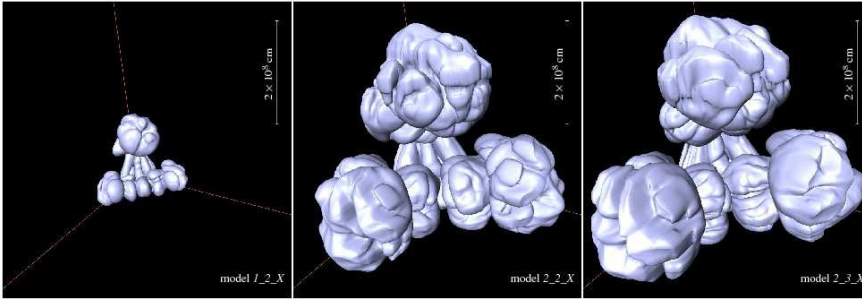


Figure 6: Snapshots of the flame front evolution at $t = 1.0$ s after ignition from models with $\rho_c = 1.0 \times 10^9 \text{ g cm}^{-3}$ and $X(^{12}\text{C}) = 0.42$ (left); $\rho_c = 2.6 \times 10^9 \text{ g cm}^{-3}$ and $X(^{12}\text{C}) = 0.42$ (middle); $\rho_c = 2.6 \times 10^9 \text{ g cm}^{-3}$ and $X(^{12}\text{C}) = 0.62$ (right)

to study effects of physical parameters on the explosion models. Such an approach was recently taken by Röpke et al. (2005a) and resulted in the first systematic study of progenitor parameters in 3D models. The basis of this study was a single-octant setup with moderate (yet numerically converged) resolution. However, the lack in resolution did not allow a reasonable multi-spot ignition scenario and thus only weak explosions can be expected. It was therefore not possible to set the absolute scale of effects in this approach, but trends can clearly be identified.

The parameters chosen for the study were the WD's carbon-to-oxygen ratio, its central density at ignition and its ^{22}Ne mass fraction resulting from the metallicity of the progenitor. All parameters were varied independently to study the individual effects on the explosion process. In a realistic scenario, however, these parameters are interrelated by the evolution of the progenitor binary system. The results of this survey are given in Tab. 1.

A variation of the carbon-to-oxygen ratio affects the energy production in the burning due to the differences in the binding energies of these two nuclei. Counter-intuitively, this results in no significant change in the ^{56}Ni production. This finding is consistent with the flame very similar flame evolution in simulations with different carbon mass fraction of the WD (cf. Fig. 6). Röpke & Hillebrandt (2004) explained this effect by the fact that the potentially higher energy release in carbon-rich models is buffered by a higher α -particle fraction in the NSE material and only released when burning is already incomplete.

Models with lower central densities show a delayed flame evolution (see Fig. 6) and consequently a lower and delayed energy production. This is due to the fact that the flame experiences a lower gravitational acceleration in these models resulting in decreased turbulence generation. Therefore less ^{56}Ni is produced in these models. This effect is even more pronounced due to the fact that in low-density WDs less material is present at sufficient densities to be potentially burnt to NSE. A counteractive effect is expected at higher densities. Here, electron captures will become important favoring neutron-rich isotopes over ^{56}Ni in the NSE. The dynamical effects of electron captures are, however, not yet implemented in the explosion model and therefore the survey of Röpke et al. (2005a) is restricted to relatively low central densities.

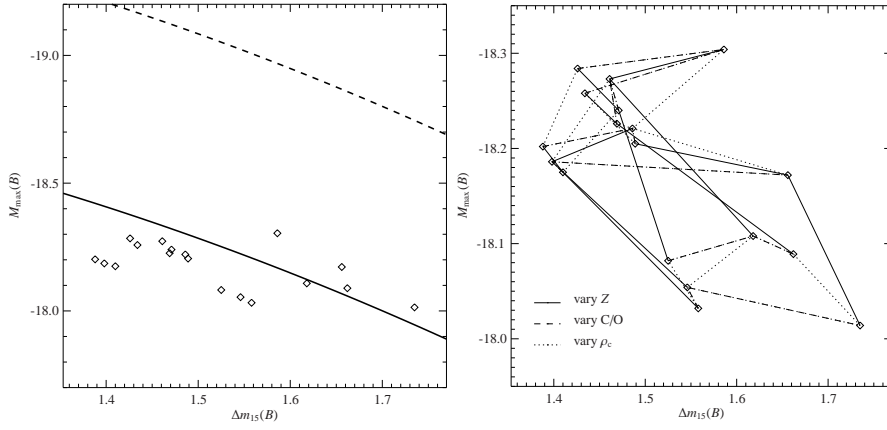


Figure 7: Peak luminosity vs. decline rate of the light curve in the B band (diamonds correspond to SN Ia explosion models). Compared with original relation by Phillips et al. (1999) (dashed curve) and shifted relation (solid curve) in the left panel.

A higher metallicity of the main sequence progenitor star results in an increased ^{22}Ne mass fraction in the WD. This is an isotope with neutron excess and therefore again favors the production of neutron-rich species over ^{56}Ni in the NSE. The results of Röpke et al. (2005a) confirm the analytic prediction by Timmes et al. (2003) and agree with Travaglio et al. (2005). The metallicity parameter, however, has no effect on the explosion dynamics and the energy production in the models.

To determine the effects of these variations on observables, synthetic light curves were derived from all models (an example is shown in Fig. 4). From these, the peak luminosities and decline rates (in magnitudes 15 days after maximum; Δm_{15}), were determined. The pioneering work by Phillips (1993) established the relation between the peak luminosity and Δm_{15} as one of the primary tools to calibrate cosmological SN Ia distance measurements. The so-called *Phillips relation* quantifies the decrease of Δm_{15} for brighter SNe Ia.

The results from the presented deflagration models are compared with the relation given by Phillips et al. (1999) in Fig. 7. Obviously, the absolute magnitude of the Phillips et al. (1999) relation is not met by the set of models (cf. the upper panel of Fig. 7). Moreover, the range of scatter in Δm_{15} is much narrower than that of the set of observations used by Phillips et al. (1999). The simulations exhibit a large scatter but are consistent with the slope of the Phillips et al. (1999) relation. It is, however, obvious, that a better agreement cannot be expected given the fact, that the parameters in the survey were chosen independently. A consistent stellar evolution would pick a sub-sample of the set of models possibly narrowing the range of scatter.

Nonetheless, with the set of models, the question can be answered, which parameter dominates the slope in the direction of dimmer events for faster decline rates. The varied parameters are coded by different line styles in the right panel of Fig. 7. Clearly, the progenitor's metallicity can be identified as this parameter. Variations in

the central density and the carbon mass fraction of the WD superpose a scatter on the dominant relation.

5 Conclusions

The rapid development of multi-dimensional SN Ia models over the past years led to a better understanding of the mechanism of these events. In particular, it has been shown, that 3D SN Ia simulations on the basis of the deflagration model are capable of reproducing main features of observed SNe Ia. However, currently it seems that they can only account for the weaker objects. A better determination of the initial conditions, i.e. the progenitor evolution and flame ignition, may improve the situation. It may, however, also turn out that the current model is incomplete. A delayed detonation was suggested by several authors to improve the agreement with observations, lacking however a convincing mechanism for a deflagration-to-detonation.

On the exemplary case of a particular numerical implementation of the deflagration scenario it was shown how such a model can be validated against observations and applied to determine the origin of the diversity of SNe Ia as a first step to theoretically assess the empirical relations utilized in SN Ia cosmology.

References

- Arnett, D. & Livne, E. 1994a, *ApJ*, 427, 315
- Arnett, D. & Livne, E. 1994b, *ApJ*, 427, 330
- Arnett, W. D. 1969, *Ap&SS*, 5, 180
- Arnett, W. D., Truran, J. W., & Woosley, S. E. 1971, *ApJ*, 165, 87
- Astier, P., Guy, J., Regnault, N., et al. 2005, [arXiv:astro-ph/0510447](https://arxiv.org/abs/astro-ph/0510447)
- Bell, J. B., Day, M. S., Rendleman, C. A., Woosley, S. E., & Zingale, M. 2004a, *J. Comp. Phys.*, 195
- Bell, J. B., Day, M. S., Rendleman, C. A., Woosley, S. E., & Zingale, M. 2004b, *ApJ*, 606, 1029
- Bell, J. B., Day, M. S., Rendleman, C. A., Woosley, S. E., & Zingale, M. 2004c, *ApJ*, 608, 883
- Blinnikov, S. I., Eastman, R., Bartunov, O. S., Popolitov, V. A., & Woosley, S. E. 1998, *ApJ*, 496, 454
- Blinnikov, S. I. & Khokhlov, A. M. 1986, *Soviet Astronomy Letters*, 12, 131
- Blinnikov, S. I., Röpke, F. K., Sorokina, E. I., et al. 2005, submitted to *A&A*
- Blinnikov, S. I. & Sasorov, P. V. 1996, *Phys. Rev. E*, 53, 4827

- Blinnikov, S. I. & Sorokina, E. I. 2000, A&A, 356, L30
- Brachwitz, F., Dean, D. J., Hix, W. R., et al. 2000, ApJ, 536, 934
- Branch, D. 1998, ARA&A, 36, 17
- Branch, D., Fisher, A., & Nugent, P. 1993, AJ, 106, 2383
- Branch, D. & Tammann, G. A. 1992, ARA&A, 30, 359
- Bravo, E., Dominguez, I., Isern, J., et al. 1993, A&A, 269, 187
- Bravo, E., Tornambe, A., Dominguez, I., & Isern, J. 1996, A&A, 306, 811
- Calder, A. C., Plewa, T., Vladimirova, N., Lamb, D. Q., & Truran, J. W. 2004, astro-ph/0405126
- Clement, M. J. 1993, ApJ, 406, 651
- Colella, P. & Woodward, P. R. 1984, J. Comp. Phys., 54, 174
- Colgate, S. A. & McKee, C. 1969, ApJ, 157, 623
- Contardo, G., Leibundgut, B., & Vacca, W. D. 2000, A&A, 359, 876
- Damköhler, G. 1940, Z. f. Elektroch., 46, 601
- Darrius, G. 1938, communication presented at *La Technique Moderne*, Unpublished.
- Domínguez, I. & Höflich, P. 2000, ApJ, 528, 854
- Domínguez, I., Höflich, P., & Straniero, O. 2001, ApJ, 557, 279
- Domínguez, I., Höflich, P., Straniero, O., & Wheeler, C. 2000, Mem. Soc. Astron. Italiana, 71, 449
- Drenkhahn, G. & Richtler, T. 1999, A&A, 349, 877
- Dursi, L. J., Zingale, M., Calder, A. C., et al. 2003, ApJ, 595, 955
- Filippenko, A. V. 1997a, ARA&A, 35, 309
- Filippenko, A. V. 1997b, in NATO ASIC Proc. 486: Thermonuclear Supernovae, ed. P. Ruiz-Lapuente, R. Canal, & J. Isern (Dordrecht: Kluwer Academic Publishers), 1–32
- Filippenko, A. V., Richmond, M. W., Branch, D., et al. 1992a, AJ, 104, 1543
- Filippenko, A. V., Richmond, M. W., Matheson, T., et al. 1992b, ApJ, 384, L15
- François, P., Matteucci, F., Cayrel, R., et al. 2004, A&A, 421, 613
- Fryxell, B. A., Müller, E., & Arnett, W. D. 1989, Hydrodynamics and nuclear burning, MPA Green Report 449, Max-Planck-Institut für Astrophysik, Garching
- Gamezo, V. N., Khokhlov, A. M., & Oran, E. S. 2004, Phys. Rev. Lett., 92, 211102
- Gamezo, V. N., Khokhlov, A. M., & Oran, E. S. 2005, ApJ, 623, 337

- Gamezo, V. N., Khokhlov, A. M., Oran, E. S., Chtchelkanova, A. Y., & Rosenberg, R. O. 2003, *Science*, 299, 77
- García-Senz, D. & Bravo, E. 2005, *A&A*, 430, 585
- García-Senz, D., Bravo, E., & Serichol, N. 1998, *ApJS*, 115, 119
- García-Senz, D. & Woosley, S. E. 1995, *ApJ*, 454, 895
- Golombek, I. & Niemeyer, J. C. 2005, *A&A*, 438, 611
- Hamuy, M., Phillips, M. M., Suntzeff, N. B., et al. 1996, *AJ*, 112, 2398
- Hansen, C. J. & Wheeler, J. C. 1969, *Ap&SS*, 3, 464
- Hillebrandt, W. & Niemeyer, J. C. 2000, *ARA&A*, 38, 191
- Hillebrandt, W., Reinecke, M., & Niemeyer, J. C. 2000, in *Proceedings of the XXXVth rencontres de Moriond: Energy densities in the universe*, ed. R. Anzari, Y. Giraud-Héraud, & J. Trân Thanh Vân (Thế Giới Publishers), 187–195
- Hillebrandt, W., Reinecke, M., Schmidt, W., et al. 2005, in *Analysis and Numerics for Conservation Laws*, ed. G. Warnecke (Berlin Heidelberg New York: Springer), 363–384, preprint available: astro-ph/0405209
- Höflich, P. & Khokhlov, A. 1996, *ApJ*, 457, 500
- Höflich, P. & Stein, J. 2002, *ApJ*, 568, 779
- Höflich, P., Wheeler, J. C., & Thielemann, F. K. 1998, *ApJ*, 495, 617
- Hoyle, F. & Fowler, W. A. 1960, *ApJ*, 132, 565
- Iapichino, L., Brüggén, M., Hillebrandt, W., & Niemeyer, J. C. 2005, arXiv:astro-ph/0512300
- Iben, I. & Tutukov, A. V. 1984, *ApJS*, 54, 335
- Ivanova, L. N., Imshennik, V. S., & Chechetkin, V. M. 1974, *Ap&SS*, 31, 497
- Iwamoto, K., Brachwitz, F., Nomoto, K., et al. 1999, *ApJS*, 125, 439
- Jeffery, D. J., Leibundgut, B., Kirshner, R. P., et al. 1992, *ApJ*, 397, 304
- Kahabka, P. & van den Heuvel, E. P. J. 1997, *ARA&A*, 35, 69
- Khokhlov, A. 1993, *ApJ*, 419, L77
- Khokhlov, A. 1994, *ApJ*, 424, L115
- Khokhlov, A. M. 1991a, *A&A*, 245, 114
- Khokhlov, A. M. 1991b, *A&A*, 245, L25
- Khokhlov, A. M. 1995, *ApJ*, 449, 695
- Kozma, C., Fransson, C., Hillebrandt, W., et al. 2005, *A&A*, 437, 983
- Kuhlen, M., Woosley, S. E., & Glatzmaier, G. A. 2005, arXiv:astro-ph/0509367

- Landau, L. D. 1944, *Acta Physicochim. URSS*, 19, 77
- Landau, L. D. & Lifshitz, E. M. 1959, *Course of Theoretical Physics, Vol. 6, Fluid Mechanics* (Oxford: Pergamon Press)
- Leibundgut, B. 2001, *ARA&A*, 39, 67
- Leibundgut, B., Kirshner, R. P., Phillips, M. M., et al. 1993, *AJ*, 105, 301
- Lisewski, A. M., Hillebrandt, W., & Woosley, S. E. 2000a, *ApJ*, 538, 831
- Lisewski, A. M., Hillebrandt, W., Woosley, S. E., Niemeyer, J. C., & Kerstein, A. R. 2000b, *ApJ*, 537, 405
- Livne, E. 1993, *ApJ*, 406, L17
- Livne, E., Asida, S. M., & Höflich, P. 2005, *ApJ*, 632, 443
- Müller, E. & Arnett, W. D. 1982, *ApJ*, 261, L109
- Müller, E. & Arnett, W. D. 1986, *ApJ*, 307, 619
- Napiwotzki, R., Karl, C. A., Nelemans, G., et al. 2005, in *ASP Conf. Ser. 334: 14th European Workshop on White Dwarfs*, 375–380
- Niemeyer, J. C. 1999, *ApJ*, 523, L57
- Niemeyer, J. C., Bushe, W. K., & Ruetsch, G. R. 1999, *ApJ*, 524, 290
- Niemeyer, J. C. & Hillebrandt, W. 1995a, *ApJ*, 452, 779
- Niemeyer, J. C. & Hillebrandt, W. 1995b, *ApJ*, 452, 769
- Niemeyer, J. C., Hillebrandt, W., & Woosley, S. E. 1996, *ApJ*, 471, 903
- Niemeyer, J. C. & Kerstein, A. R. 1997, *New Astronomy*, 2, 239
- Niemeyer, J. C. & Woosley, S. E. 1997, *ApJ*, 475, 740
- Nomoto, K. 1982, *ApJ*, 253, 798
- Nomoto, K. & Iben, I. 1985, *ApJ*, 297, 531
- Nomoto, K., Sugimoto, D., & Neo, S. 1976, *Ap&SS*, 39, L37
- Nomoto, K., Thielemann, F.-K., & Yokoi, K. 1984, *ApJ*, 286, 644
- Oran, E. S. & Boris, J. P. 1987, *Numerical simulation of reactive flow* (New York: Elsevier)
- Osher, S. & Sethian, J. A. 1988, *J. Comp. Phys.*, 79, 12
- Perlmutter, S., Aldering, G., Goldhaber, G., et al. 1999, *ApJ*, 517, 565
- Peters, N. 2000, *Turbulent Combustion* (Cambridge: Cambridge University Press)
- Phillips, M. M. 1993, *ApJ*, 413, L105
- Phillips, M. M., Lira, P., Suntzeff, N. B., et al. 1999, *AJ*, 118, 1766

Phillips, M. M., Wells, L. A., Suntzeff, N. B., et al. 1992, *AJ*, 103, 1632

Plewa, T., Calder, A. C., & Lamb, D. Q. 2004, *ApJ*, 612, L37

Reinecke, M., Hillebrandt, W., & Niemeyer, J. C. 1999a, *A&A*, 347, 739

Reinecke, M., Hillebrandt, W., & Niemeyer, J. C. 2002a, *A&A*, 386, 936

Reinecke, M., Hillebrandt, W., & Niemeyer, J. C. 2002b, *A&A*, 391, 1167

Reinecke, M., Hillebrandt, W., Niemeyer, J. C., Klein, R., & Gröbl, A. 1999b, *A&A*, 347, 724

Reinecke, M., Niemeyer, J. C., & Hillebrandt, W. 2002c, *New Astronomy Review*, 46, 481

Riess, A. G., Filippenko, A. V., Challis, P., et al. 1998, *AJ*, 116, 1009

Röpke, F. K. 2005, *A&A*, 432, 969

Röpke, F. K., Gieseler, M., Reinecke, M., Travaglio, C., & Hillebrandt, W. 2005a, *A&A* in print, preprint available: astro-ph/0506107

Röpke, F. K. & Hillebrandt, W. 2004, *A&A*, 420, L1

Röpke, F. K. & Hillebrandt, W. 2005a, *A&A*, 431, 635

Röpke, F. K. & Hillebrandt, W. 2005b, *A&A*, 429, L29

Röpke, F. K., Hillebrandt, W., & Niemeyer, J. C. 2004a, *A&A*, 420, 411

Röpke, F. K., Hillebrandt, W., & Niemeyer, J. C. 2004b, *A&A*, 421, 783

Röpke, F. K., Hillebrandt, W., Niemeyer, J. C., & Woosley, S. E. 2006a, *A&A*, 448, 1

Röpke, F. K. et al. 2006b, in preparation

Röpke, F. K., Niemeyer, J. C., & Hillebrandt, W. 2003, *ApJ*, 588, 952

Ruiz-Lapuente, P., Cappellaro, E., Turatto, M., et al. 1992, *ApJ*, 387, L33

Ruiz-Lapuente, P., Comeron, F., Méndez, J., et al. 2004, *Nature*, 431, 1069

Saio, H. & Nomoto, K. 1985, *A&A*, 150, L21

Saio, H. & Nomoto, K. 1998, *ApJ*, 500, 388

Schmidt, W., Hillebrandt, W., & Niemeyer, J. C. 2005a, *Combustion Theory and Modelling*, 9, 693

Schmidt, W. & Niemeyer, J. C. 2006, *A&A*, 446, 627

Schmidt, W., Niemeyer, J. C., & Hillebrandt, W. 2005b, *A&A* in print, preprint available: astro-ph/0601499

Schmidt, W., Niemeyer, J. C., Hillebrandt, W., & Röpke, F. K. 2005c, *A&A* in print, preprint available: astro-ph/0601500

Sethian, J. A. 1996, *Level Set Methods* (Cambridge: University Press)

Sharpe, G. J. 1999, MNRAS, 310, 1039

Smiljanovski, V., Moser, V., & Klein, R. 1997, *Combustion Theory and Modelling*, 1, 183

Sollerman, J., Aguilera, C., Becker, A., et al. 2005, arXiv:astro-ph/0510026

Sorokina, E. & Blinnikov, S. 2003, in *From Twilight to Highlight: The Physics of Supernovae*, ed. W. Hillebrandt & B. Leibundgut, ESO Astrophysics Symposia (Berlin Heidelberg: Springer-Verlag), 268–275

Spergel, D. N., Verde, L., Peiris, H. V., et al. 2003, ApJS, 148, 175

Spyromilio, J., Meikle, W. P. S., Allen, D. A., & Graham, J. R. 1992, MNRAS, 258, 53P

Stehle, M., Mazzali, P. A., Benetti, S., & Hillebrandt, W. 2005, MNRAS, 360, 1231

Steinmetz, M., Muller, E., & Hillebrandt, W. 1992, A&A, 254, 177

Stritzinger, M., Leibundgut, B., Walch, S., & Contardo, G. 2005, arXiv:astro-ph/0506415

Thielemann, F.-K., Nomoto, K., & Yokoi, K. 1986, A&A, 158, 17

Timmes, F. X., Brown, E. F., & Truran, J. W. 2003, ApJ, 590, L83

Timmes, F. X. & Woosley, S. E. 1992, ApJ, 396

Travaglio, C., Hillebrandt, W., & Reinecke, M. 2005, A&A, 443, 1007

Travaglio, C., Hillebrandt, W., Reinecke, M., & Thielemann, F.-K. 2004, A&A, 425, 1029

Truran, J. W., Arnett, W. D., & Cameron, A. G. W. 1967, *Canad. J. Physics*, 45, 2315

Umeda, H., Nomoto, K., Kobayashi, C., Hachisu, I., & Kato, M. 1999, ApJ, 522, L43

Wang, L., Baade, D., Höflich, P., et al. 2003, ApJ, 591, 1110

Webbink, R. F. 1984, ApJ, 277, 355

Wheeler, J. C. & Harkness, R. P. 1990, *Reports of Progress in Physics*, 53, 1467

Whelan, J. & Iben, I. J. 1973, ApJ, 186, 1007

Woosley, S. E. 1990, in *Supernovae*, ed. A. G. Petschek (New York: Springer-Verlag), 182–212

Woosley, S. E. & Weaver, T. A. 1994, in *Les Houches Session LIV: Supernovae*, ed. S. Bludman, R. Mochovitch, & J. Zinn-Justin (Amsterdam: North-Holland), 63–154

Woosley, S. E., Wunsch, S., & Kuhlen, M. 2004, ApJ, 607, 921

Zel'dovich, Y. B. 1966, *Journal of Appl. Mech. and Tech. Physics*, 1, 68, english translation

Zingale, M., Woosley, S. E., Rendleman, C. A., Day, M. S., & Bell, J. B. 2005, ApJ, 632, 1021

Zwicky, F. 1938, ApJ, 88, 522